Journal of Applied Polymer Science

Development and Characterization of Gelatin-Based Hydrogels, Emulsion Hydrogels, and Bigels: A Comparative Study

Sitipragyan Satapathy,[1] Vinay K. Singh,[1] Sai Sateesh Sagiri,[1] Tarun Agarwal,[1] Indranil Banerjee,[1] Mrinal K. Bhattacharya,[2] Naresh Kumar,[3] Kunal Pal[1]

[1]Department of Biotechnology and Medical Engineering, National Institute of Technology, Rourkela, India

[2]Department of Botany & Biotechnology, Karimganj College, Karimganj, Assam, India

[3]Scientific and Digital Systems, IDA House, New Delhi, India

Correspondence to: K. Pal (E-mail: pal.kunal@yahoo.com or kpal.nitrkl@gmail.com)

ABSTRACT: This study was designed to examine the physicochemical and electrical properties of gelatin-based hydrogels, emulgels, and bigels. The chemical studies suggested an increase in hydrogen bonding in the emulgel and bigel when sesame oil (SO; representative vegetable oil) and SO organogel (OG; representative OG) were incorporated within the gelatin matrix. The emulgel and bigel showed better mechanical properties and higher electrical impedances compared to the hydrogel. The hydrogel showed similar swelling at pH 1.2 and 7.2. The swelling of the emulgel and bigel was higher at pH 7.2. The formulations were found to be highly hemocompatible; this indicated their biocompatible nature. Ciprofloxacin, a model antimicrobial drug, was incorporated within the formulations. The release of the drug was found to be diffusion-mediated. The antimicrobial efficiency of all of the drug-loaded formulations was found to be equivalent. © 2014 Wiley Periodicals, Inc. J. Appl. Polym. Sci. **2015**, *132*, 41502.

KEYWORDS: biocompatibility; drug-delivery systems; gels

Received 28 May 2014; accepted 4 September 2014

DOI: 10.1002/app.41502

INTRODUCTION

Gels are defined as semisolid formulations. They are usually made up of two components, namely, a solid component (gelator) and a liquid component (aqueous or nonaqueous).[1] The solid molecules form a three-dimensional network in which the liquid molecules are entrapped.[2] If the liquid is aqueous, the gels are regarded as hydrogels; otherwise, they are regarded as organogels (OGs). In the past decade, there has been extensive work on hydrogel-based systems.[3] Hydrogels may be defined as polymeric architectures having the capability to imbibe and hold water within their structures. Hydrogels have been reported to be mucoadhesive in nature, and this depends on the composition of the polymer matrix. Mucoadhesive hydrogels help to deliver drugs to the site of action for prolonged periods. This allows increased bioavailability of the drug.[4] Apart from the mucoadhesive properties, hydrogels have been reported to alter the release kinetics of drugs to form controlled delivery matrices by tailoring the crosslinking density of the hydrogels.[5] In the past decade, researchers have introduced *emulgels* (emulsion gels) as controlled delivery vehicles with improved characteristics.[6] Emulgels are biphasic systems like emulsions. However, the external phase of emulgels is semisolid in nature, unlike emulsions; this helps to improve the thermodynamic stability of the emulgels.[7] This results in the formation of semisolid formulations, which have the combined advantages of emulsions (controlled release) and gels (thermodynamic stability). Unfortunately, the leaching of the internal oil phase during long-term storage has forced scientists to look for better formulations that can be stable during long-term storage.[8] This problem may be attributed to the mismatch in the mechanical properties of the internal and the external phases. To overcome this problem, recently, the concept of bigels was introduced. *Bigels* are biphasic systems like emulsions and emulgels, but unlike those in emulsions and emulgels, both phases (internal and external) are semisolid in nature.

To date, no reports on the comparison of the properties of these three types formulations were found. Taking a note of this, we tried to develop a gelatin-based hydrogel, an emulgel, and a bigel and thoroughly characterized their properties. The main aim of this study was to check whether the bigel could be prepared with the composition of that of the hydrogel and emulgel. When it formed, the physicochemical, thermal, and mechanical properties of the bigel were checked against those of the hydrogel and emulgel. In addition to the characterization, the

Additional Supporting Information may be found in the online version of this article.

Table I. Compositions of the Developed Formulations

Sample code	GS (g)	SO (g)	OG (g)	Tween 80 (g)	Ciprofloxacin (g)
G1	20.0	—	—	—	—
G1C	19.8	—	—	—	0.2
G2	17.5	2.5	—	0.5	—
G2C	17.3	2.5	—	0.5	0.2
G3	17.5	—	—	0.5	—
G3C	17.3	—	2.5	0.5	0.2

suitability of the formulations for *in vitro* drug-release studies was analyzed by the loading of ciprofloxacin as the model drug. The efficacy of the antimicrobial effect of the drug-loaded formulations was tested against *E. coli*. Sesame oil (SO) was used for the development of the emulgels and bigels. It was obtained from the seeds of *Sesamum indicum*. Span 60 (sorbitan monostearate) was used as the gelator for SO for the preparation of the OG (internal phase of bigel). Span 60 is an ester of sorbitan and stearic acid. Span 60 was used as an emulsifier because of its nonionic surfactant nature. Span 60 is a generally-regarded-as-safe emulsifier and approved by the U.S. Food and Drug Administration as a food additive.[9]

EXPERIMENTAL

Materials

Gelatin and Tween 80 [poly(xyethylene sorbitan monooleate)] were procured from Himedia (Mumbai, India). Ethanol was obtained from Honyon International, Inc., Hong Yang Chemical Corp. (China). Glutaraldehyde (GA; 25% for synthesis) and hydrochloric acid (35% pure) was obtained from Merck Specialities Private, Ltd. (Mumbai, India). Span 60 was procured from Loba Chemie (Mumbai, India). SO (Tilsona, Recon Oil Industries Pvt., Ltd., Mumbai, India) was obtained from the local market. Goat intestine and blood were obtained from a local butcher shop. Double-distilled water was used throughout the study. Ciprofloxacin was procured from Fluka (China). *E. coli* (NCIM 2563) was purchased from NCIM (Pune, India).

Methods

Preparation of the Hydrogel. A twenty percent (w/w) gelatin solution (GS) was prepared by the dissolution of 20 g of gelatin in 70 g of water, whose temperature was maintained at 70°C; it was stirred at 600 rpm to obtain a clear homogeneous solution. After homogenization, the final mass of the GS was made to 100 g by the addition of water.

Preparation of the Emulgel. The emulgel was prepared as per a protocol reported earlier.[10] In brief, 2.5 g of SO was slowly added to a mixture of 0.5 g of Tween 80 and 17. 5 g of the previously prepared GS and maintained at 70°C (600 rpm, magnetic stirrer). The stirring was done for 15 min for proper homogenization. A volume of 0.5 mL of the GA reagent (2 mL of GA + 2 mL of ethanol + 0.05 mL of 0.01*N* hydrochloric acid) was added to the previous mixture, mixed for 10 s (600 rpm, 70°C), and immediately poured in either Petri plates or cylindrical molds. The Petri plates/molds were incubated at 37°C for 30 min to induce the gelation and formation of emulgel.

Preparation of the OG. The SO OG was prepared by the dissolution of 1.5 g of Span 60 in 8.5 g of SO and maintained at 70°C (100 rpm).[11] The hot homogeneous solution, so formed, was kept under room temperature (25°C) to form OG.

Preparation of the Bigel. The bigel was prepared as per the methodology described for emulgels with a slight modification. SO-based OG, maintained at 70°C, was used instead of SO for the preparation of the bigel. The rest of the procedure remained the same.

After the preparation, the formulations (hydrogel, emulgel, and bigel) were critically observed visually and their texture was observed by touching with bare hands.

Preparation of the Drug-Loaded Samples. The drug-loaded hydrogel, emulgel, and bigel were prepared in a similar manner. Ciprofloxacin was dispersed in GS to prepare the drug-loaded hydrogel.[12] The drug was dispersed in SO and SO OG to prepare the drug-loaded emulgel and bigel, respectively. The final concentration of ciprofloxacin in the formulations was 1% w/w. The compositions of the formulations are tabulated in Table I.

Microscopic Studies. Bright-field microscopy was performed when the formulations were in their liquid state. Because the crosslinker was added to each of the formulations, microscopy was performed with the samples before the addition of the crosslinker. The liquid GS, emulgel, and bigel formulations were put over a glass slide and converted into thin smears. The thin smears were studied under bright-field microscopy (CH20i, Olympus, India).[13]

The surface morphology of the formulations was studied under field emission scanning electron microscopy (FESEM; Nova NanoSEM) after they were converted into xerogels. The formulations were dried for 72 h (40°C) to convert the formulations into xerogels. The xerogels were sputter-coated with platinum before analysis.[14]

Molecular Interaction Studies. The formulations were cut into pieces 1 × 1 cm^2 and were analyzed with an X-ray diffractometer (XRD-PW 1700, Philips, Rockville, MD).The X-ray radiation source was Cu Kα and was operated at 30 kV and 20 mA.[15] The scanning was done in the diffraction angle ranges of 5–50° at a rate of 2°/min.

The chemical interactions among the components of the formulations were studied with Fourier transform infrared (FTIR)

Table II. Instrumental Parameters of the Textural Analyses

Type of study	Type of fixture	Testing condition: Pretest speed (mm/s)	Testing condition: Test speed (mm/s)	Testing condition: Posttest speed (mm/s)	Mode of study
SR	P/30 flat probe, 30-mm diameter	1.0	1.0	1.0	Auto force (5 g), target distance = 5 mm
Creep recovery	P/30 flat probe, 30-mm diameter	1.0	1.0	1.0	Creep stages: 200 g and 5 min, recovery stages: 5 g and 5 min, cycles = 10

spectroscopy (Alfa-E, Bruker, Germany) working in the ATR mode. The scanning was done in the wave-number range of 500–4000 cm^{-1}.[16]

Swelling Studies. The swelling profile of the formulations were checked under acidic (HCl buffer, pH 1.2) and basic (phosphate buffer, pH 7.2) conditions. The formulations were cut into pieces of 1 × 1 cm^2. The pieces were weighed accurately and immersed in 50 mL of buffer. The samples were taken out of the buffers at regular intervals of 30 min for the first 1 h and 1 h thereafter for 7 h.[17] The surface moisture of the formulation pieces was removed with Whatmann paper and weighed accurately (W_t). The percentage swelling ratio was calculated by the following equation:

$$\text{Swelling}(\%) = \frac{W_t - W_i}{W_i} \times 100 \quad (1)$$

where W_i is the initial mass of the gel and W_t is the mass of the swollen gel.

Mucoadhesion Studies. The mucoadhesive properties of the formulations were tested with a wash-off method and a mechanical tester. Goat intestinal mucosa was used for the study. Mucoadhesion with a wash-off method was conducted in a tablet disintegration apparatus. The intestinal lumen was cut open and attached to glass slides, such that the intestinal mucosa was exposed outward with a commercially available acrylate adhesive. Formulations (5 × 5 mm^2) were put on the exposed surface of the intestinal mucosa. A mass of 5 g was applied over the formulations for 5 min. Thereafter, the slides were put vertically into USP disintegration baskets. Phosphate buffer (pH 7.2) was used as the disintegration medium. The experiment was carried out for 24 h. The setup was continuously monitored to detect the detachment of the formulations from the intestinal mucosal surface. The time required to detach the formulations from the mucosal surface was noted.[18]

The mucoadhesive strength was determined with a texture analyzer (Stable Microsystems, TA-HD Plus, United Kingdom). The formulations (5 × 5 mm^2) were attached at the surface of the cylindrical probe (30 mm in diameter) with double-sided acrylate tape.[19] The goat intestine was longitudinally cut open, cut into rectangular pieces with dimensions of 1.5 × 1.5 cm^2, and attached onto the aluminum platform of the texture analyzer with double-sided acrylate tape such that the mucosal surface was exposed. The probe (attached with hydrogels) exerted a force of 20 g at a rate of 1 mm/s for 1 min onto the intestinal mucosa. Thereafter, the probe was retracted back, and the maximum force (F_0) required to detach the hydrogels from the mucosal surface was determined.[20]

Mechanical Properties. The mechanical properties of the formulations were studied with a texture analyzer. The mechanical properties of the formulations were studied through a series of tests [stress relaxation (SR) and creep recovery] at room temperature. The experimental parameters are listed in Table II.[21]

Thermal Properties. The formulations were converted into xerogels through drying for 72 h at 40°C. Accurately weighed amounts of about 10–15 mg of the xerogels were put into aluminum pans and hermitically sealed with pierced aluminum lids. The thermal analysis was done in the temperature range 20–150°C at a heating rate of 2°C/min under a nitrogen atmosphere in a differential scanning calorimeter (DSC 200 F3 Maia, Netzsch, Germany).[22,23]

Impedance Analysis. The electrical properties of the formulations were tested with an impedance analyzer (HIOKI 3532–50-LCR Hitester). The analysis was done in the frequency range 50 Hz–1 MHz. An alternating-current (ac) voltage of 100 mV was used for the study. The voltage (V)–current (I) characteristics of the samples were measured with a device built in house at 10 kHz. The test was done at 10 kHz to eliminate the polarization effect at the sample electrode interface.[24,25]

Drug-Release Studies. The *in vitro* release study of ciprofloxacin was carried out as per the reported literature with slight modifications.[3] In short, circular pieces of formulations (1.9 cm in diameter) were immersed in 50 mL of dissolution media and stirred at 100 rpm (37°C). The dissolution media was HCl buffer (pH 1.2) for the first 2 h and phosphate buffer (pH 7.2) for the next 7 h. At regular intervals of time (for every 30 min in the first 1 h and then for every 1 h), the dissolution media was replaced with fresh dissolution media to maintain the sink conditions. The replaced dissolution media was analyzed spectrophotometrically at 271 nm with an ultraviolet–visible (UV–vis) spectrophotometer to determine the concentration of ciprofloxacin.[26]

The efficacy of the formulations to release the drug in its active form and inhibit the growth of the microbes was tested by an agar diffusion method. A volume of 100 μl of *E. coli* suspension

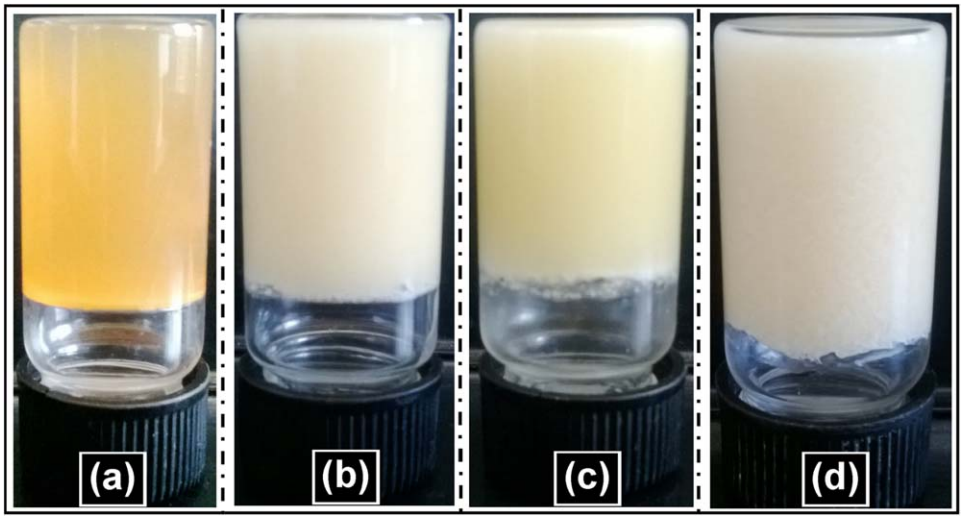

Figure 1. Pictographs of the (a) hydrogel, (b) emulgel, (c) OG, and (d) bigel. [Color figure can be viewed in the online issue, which is available at wileyonlinelibrary.com.]

(2×10^5 cfu/mL) was spread over the nutrient agar plates. The pieces (7 mm in diameter) of the formulations (with and without ciprofloxacin) were put over the agar plates. The agar plates were subsequently incubated at 37°C (12 h). The zone of inhibition of the microbe was measured with a ruler at the end of the study.[27]

Biocompatibility. The preliminary biocompatibility test of the formulations was estimated by a hemocompatibility test as per previously reported literature.[28,29] In short, citrated goat blood was diluted with normal saline (4:5 ratio). The formulations were cut into pieces 1×1 cm^2. The pieces were poured into falcon tubes. A volume of 0.5 mL of diluted blood was added to the falcon tubes followed by a sufficient amount of normal saline to make the final volume 10 mL. Positive and negative controls were prepared with 0.5 mL of 0.01*N* HCl and 0.5 mL of normal saline, respectively. The falcon tubes were then incubated at 37°C for 60 min. The falcon tubes were centrifuged at 3000 rpm for 10 min. The optical density of the supernatant was measured at 545 nm with a UV–vis spectrophotometer. The

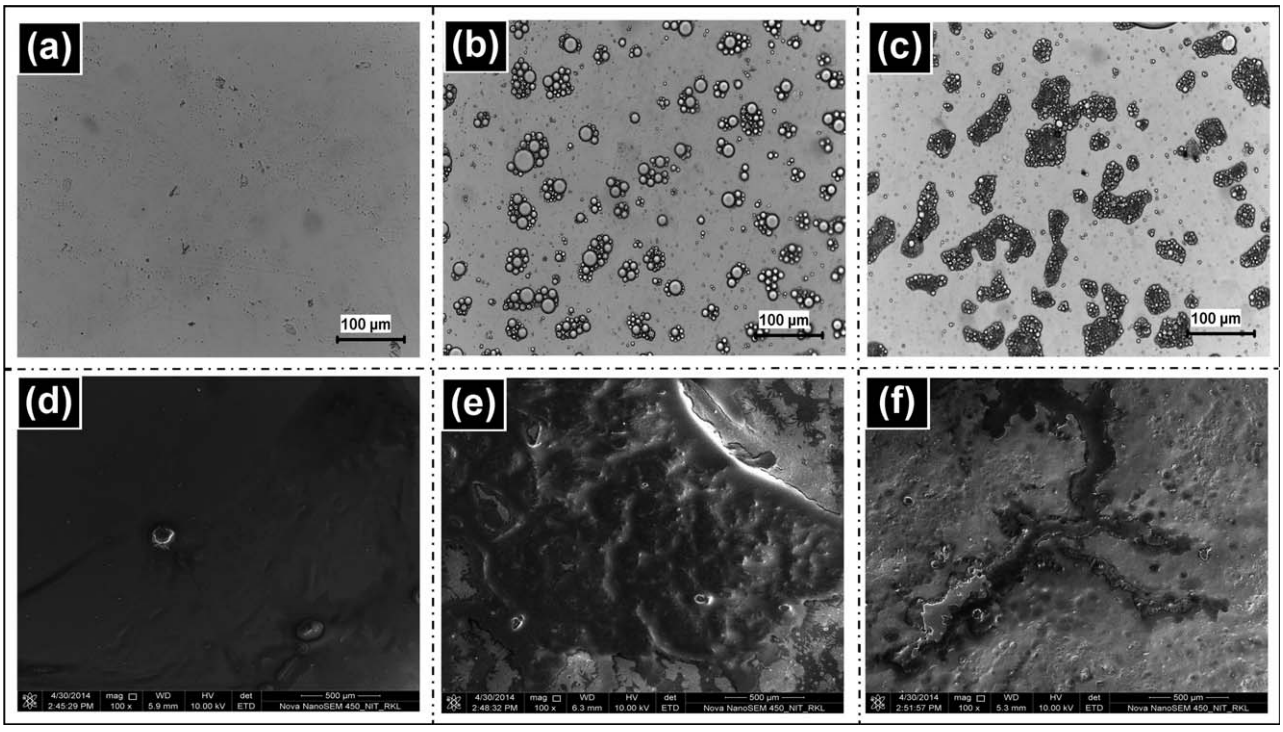

Figure 2. Bright-field micrographs of the (a) gelatin, (b) emulgel, and (c) bigel. FESEM of (d) gelatin, (e) emulgel, and (f) bigel.

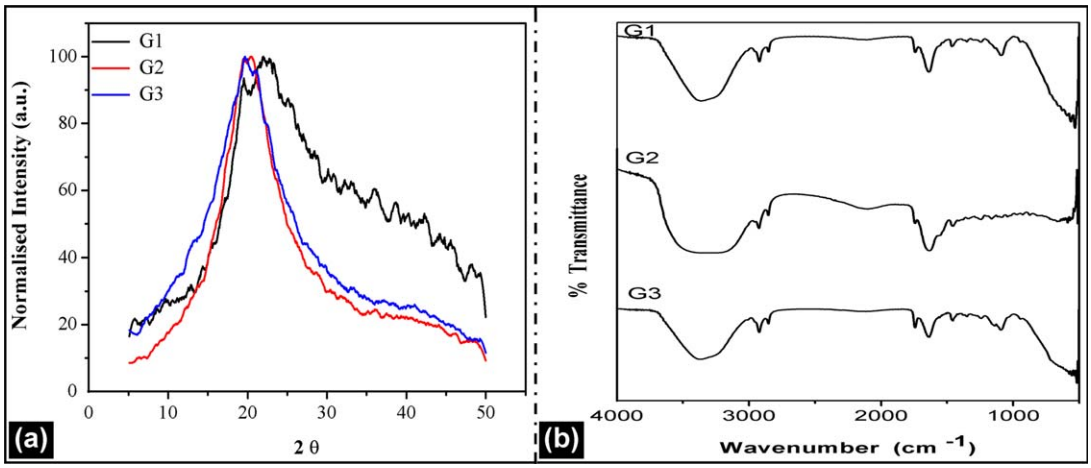

Figure 3. Molecular interactions: (a) XRD profile and (b) FTIR profile of the formulations. [Color figure can be viewed in the online issue, which is available at wileyonlinelibrary.com.]

percentage hemolysis was calculated as per the following formula:[3,30]

$$\text{Hemolysis}(\%) = \frac{\text{OD}_{\text{test}} - \text{OD}_{\text{negative}}}{\text{OD}_{\text{positive}} - \text{OD}_{\text{negative}}} \times 100 \quad (2)$$

where OD_{test} is the optical density of the test sample, $\text{OD}_{\text{positive}}$ is the optical density for the positive control, and $\text{OD}_{\text{negative}}$ is the optical density for the negative control.

The biocompatibility of the prepared formulations was evaluated with the HaCaT cell line by 3-(4,5-dimethylthiazol-2-yl)-2,5-diphenyltetrazolium bromide (MTT) assay according to a protocol described elsewhere.[31] The leachants of the formulations were prepared by the incubation of 1 g of the formulations in 30 mL of phosphate-buffered saline for 24 h at 37°C. The supernatant was used for the analysis.[32] The cells were seeded into a 96-well plate at a cell concentration of 1×10^4 cells/well and incubated at 37°C in CO_2 for 24 h. Thereafter, 20 μL of the leachants was added to each well and incubated for 24 h. The cell viability was estimated with MTT assay after 24 h.

RESULTS AND DISCUSSIONS

Preparation of the Gels

The pictographs of the gelatin hydrogel, emulgel, OG, and bigel are shown in Figure 1. The gelatin hydrogel was light brownish yellow in color and translucent. The emulgel and bigel were opaque. The emulgel was light brownish white in color. The bigel was slightly darker than the emulgel (dark borwnish white). The whitish tinge of the emulgel and the bigel could be explained by the diffraction of light from the interface of the immiscible phases (a property often associated with emulsions).[33] All of the formulations had a smooth texture and a soothing effect.

Microscopic Studies

The hot homogenized sol (gelatin) and emulsions (emulgel and bigel) were converted into thin smears and analyzed with bright-field microscopy [Figure 2(a–c)]. The microstructure of the gelatin smears did not show any definite architecture. The emulgel and the bigel showed presence of agglomerated globular structures dispersed uniformly throughout the gelatin matrix. The agglomerated dispersed phase in the bigel was irregular in size and shape.[34]

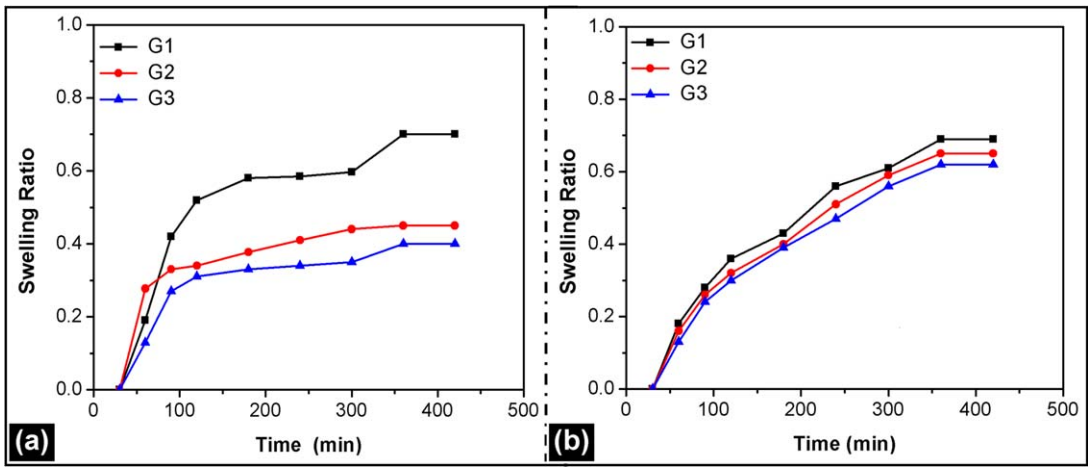

Figure 4. Swelling study at pH of (a) 1.2 and (b) 7.2. [Color figure can be viewed in the online issue, which is available at wileyonlinelibrary.com.]

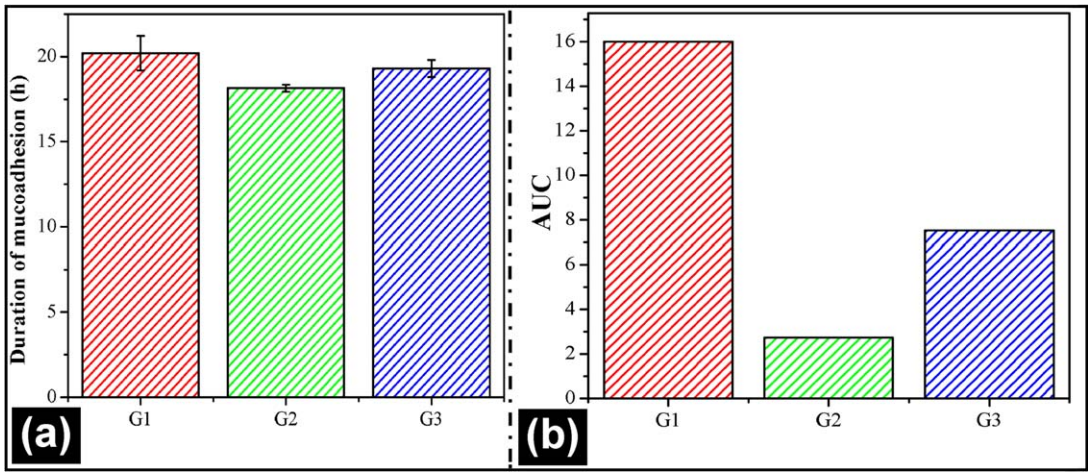

Figure 5. Mucoadhesive properties: (a) wash-off method and (b) work of adhesion by a mechanical testing method. [Color figure can be viewed in the online issue, which is available at wileyonlinelibrary.com.]

The surface topology of the formulations were studied under FESEM after the formulations were converted into xerogels [Figure 2(d–f)]. The hydrogels showed a smooth surface. This was due to the absence of any internal structures. The emulgel and bigel showed the presence of agglomerated globular structures dispersed within a polymer continuum phase. Apart from the agglomerated particles, fiberlike structures were also visible in the bigel. The micrographs of the formulations from light microscopy and FESEM were in support of each other.[35]

Molecular Interaction Studies

The normalized X-ray diffractograms of the hydrogel, emulgel, and bigel showed a broad peak at a 2θ about 20° [Figure 3(a)]. This kind of X-ray diffraction (XRD) profile is generally associated with amorphous formulations. The full width at half-maximum (fwhm) of the peaks of the diffractograms was calculated from the XRD profile (Table S1). The fwhm's were found to be in the order of G1 (hydrogel) > G3 (bigel) > G2 (emulgel). Higher fwhm values suggested a lower crystallinity (or higher amorphosity).[36] The results indicate that G2 was having higher crystallinity as compared to G3 followed by G1. The higher crystallinity of G2 and G3 as compared to that of G1 could be explained by the higher degree of hydrogen bonding of the gelatin molecules with the fatty acids present in the SO and SO OGs. G3 showed intermediate crystallinity because of the availability of the lesser number of fatty acid molecules (as compared to that in G2) for hydrogen bonding because of the interaction with Span 60. Because no fatty acid was present

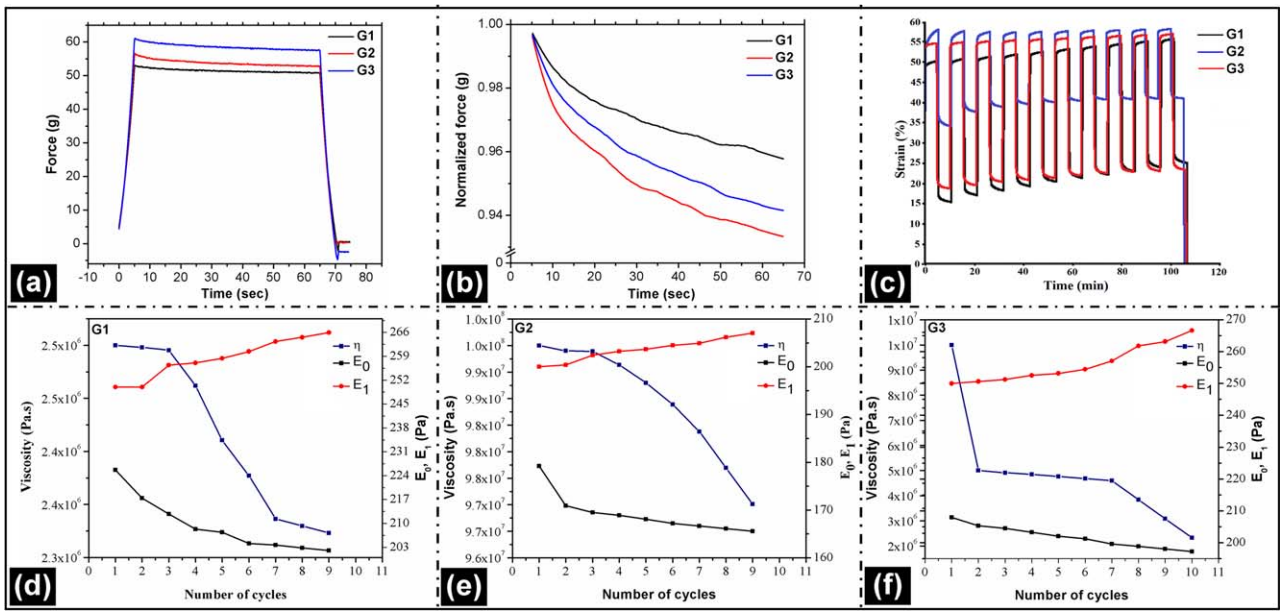

Figure 6. Mechanical properties of the formulations in the (a,b) SR study and (c) creep and recovery study. Storage modulus values of (d) G1, (e) G2, and (f) G3 (where η is viscosity, E_0 is storage modulus and E_1 is loss modulus of the formulations). [Color figure can be viewed in the online issue, which is available at wileyonlinelibrary.com.]

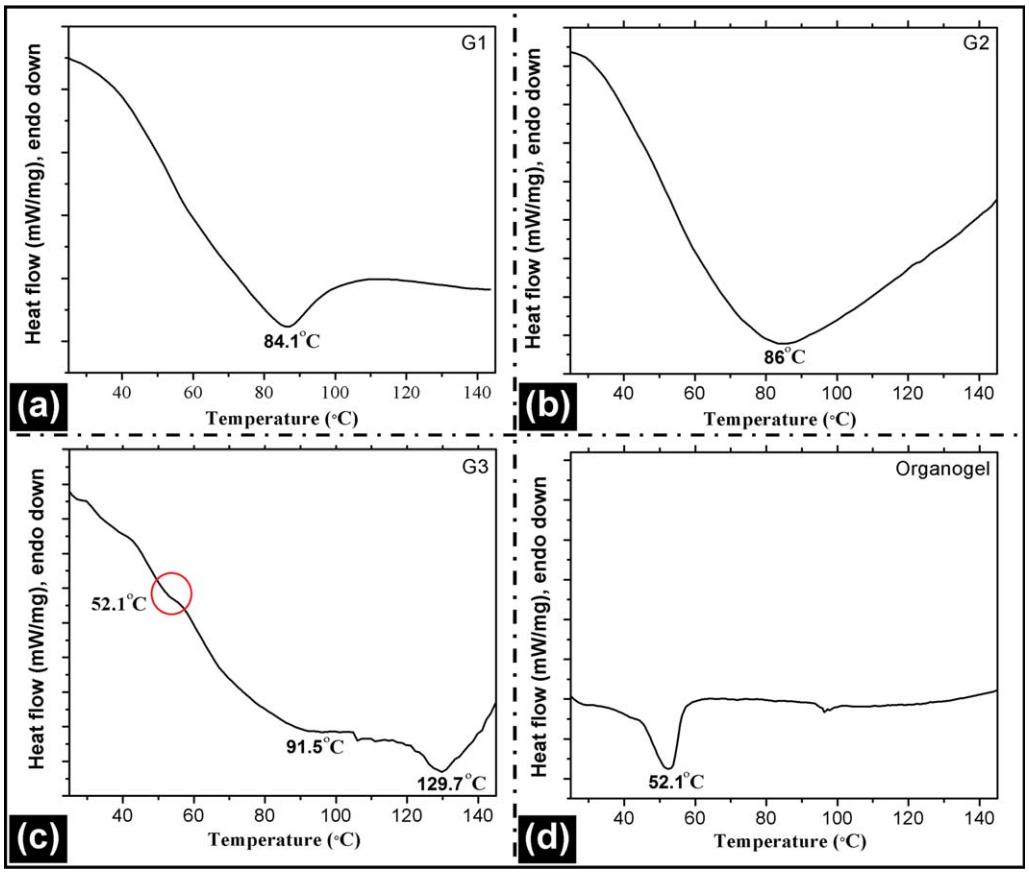

Figure 7. Thermograms of (a) G1, (b) G2, and (c) G3 and OG. [Color figure can be viewed in the online issue, which is available at wileyonlinelibrary.com.]

in G1, the degree of hydrogen bonding was lowest and so was the crystallinity. Similar results were also obtained by the FTIR studies.

The FTIR studies of the formulations were conducted to understand the interactions among the functional groups [Figure 3(b)]. The peak at about 1640 cm^{-1} was associated with the C═O stretching of the amide I bands. The peak at about 1540 cm^{-1} could be explained by the presence of amide II bands. The peak at about 3400 cm^{-1} was due to the combined O—H and N—H stretching vibrations. The formation of a broad peak in the said region suggested presence of intermolecular hydrogen bonding. The absorption peak in the region 3000–2800 cm^{-1} was due to C—H stretching vibrations.[37] The stretching vibrations of methylene (—CH_2—) and methyl (—CH_3) groups were observed at about 2920 and 2850 cm^{-1}, respectively. All of the peaks of the gelatin hydrogel were conserved in the emulgel and the bigel. The peak at about 3400 cm^{-1} was broadened in the emulgel and the bigel. This was due to the higher degree of hydrogen bonding among the fatty acid and gelatin molecules. No peaks corresponding to ciprofloxacin were observed in the drug-loaded formulations (Figure S1, Supporting Information). This could be explained by the presence of the drug in very minute concentrations, and hence, the peaks due to the drugs were completely suppressed by the strong peaks of the gelatin hydrogel matrices.

Swelling Studies

The swelling profile of the formulations were checked at pH 1.2 and 7.2. G1 showed nearly equal swelling in both the acidic and basic conditions [Figure 4(a,b)]. This may have been due to the presence of both anionic (COO^-) and cationic (NH_4^+) groups, which are present in gelatin.[38] G2 and G3 showed lower swelling in acidic pH than in basic pH. This was due to the presence of fatty acid molecules (in SO). The fatty acids did not accommodate the aqueous phase within its structure at lower pH because of an electrostatic shielding effect.[39] On the other hand, the electrostatic shielding effect was lower at pH 7.2, and hence, this allowed accommodation of the aqueous phase. The accommodation of the aqueous phase was limited by the elastic force exerted by the gelatin matrix.

Mucoadhesive Properties

The mucoadhesive properties of the formulations were tested by an *in vitro* wash-off method [Figure 5(a)] and a mechanical testing method [Figure 5(b)]. The wash-off method deals with the determination of the adhesion time of the formulations with the mucosal surface when the interface is being moved in and out of the media. The test was done in phosphate buffer (pH 7.2). The detachment times of G1, G2, and G3 were found to be 1200 ± 20, 1080 ± 15, and 1140 ± 30 min, respectively. The results indicate that the mucoadhesivity of G1 was highest, followed by G3 and G2, respectively. The encapsulation of the

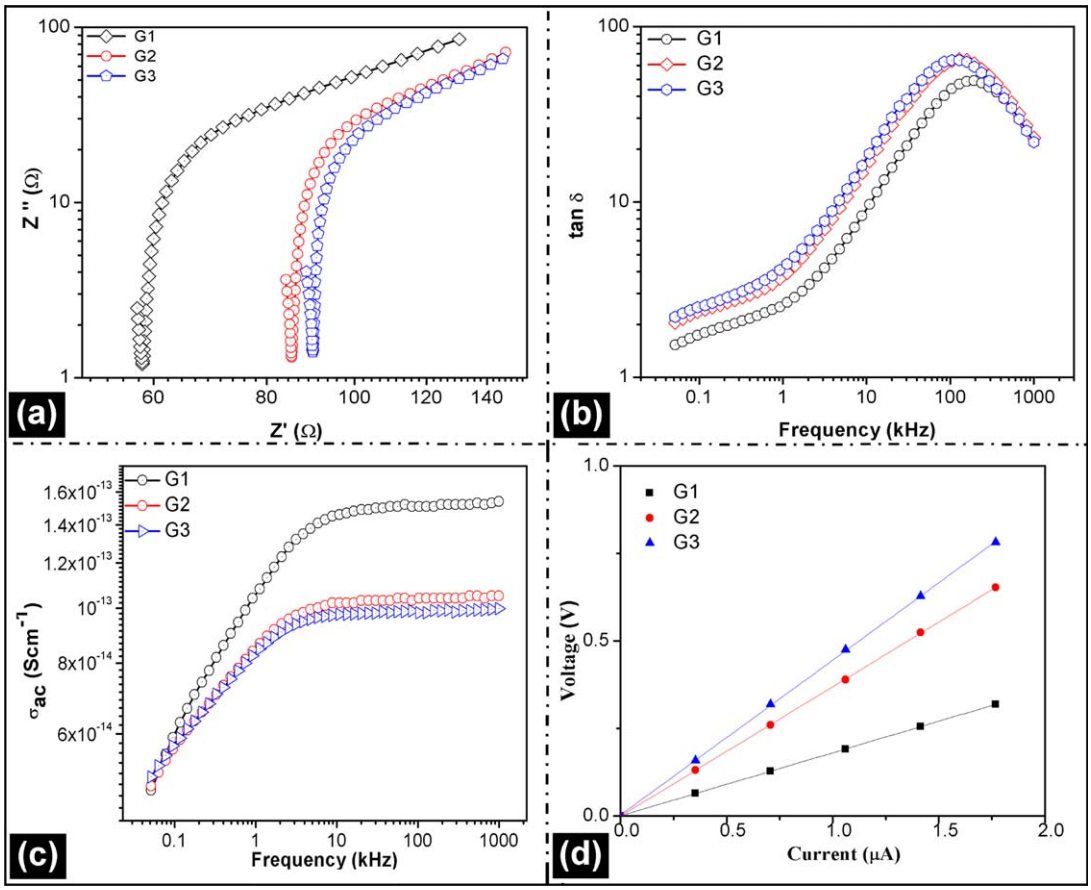

Figure 8. Electrical properties of the formulations: (a) Nyquist plot, (b) tan δ versus frequency plot, (c) σ_{ac} is the a.c. conductivity versus frequency, and (d) *V–I* characteristics plot. [Color figure can be viewed in the online issue, which is available at wileyonlinelibrary.com.]

oil and OG reduced the mucoadhesive properties. Similar results were reported earlier when oils and OGs were encapsulated within polymeric microparticles.[40] The decrease in the mucoadhesive properties was explained by the leaching of the internal phase, which altered the interaction between the formulation and the mucosal surface.

The work done to separate the formulations from the mucosal surface is regarded as the *work of adhesion*. The work of adhesion is generally calculated from the area under the curve (AUC) of the force–time (force–distance) profile. The AUCs were found to be in the order G1 > G3 > G2. The results were in accordance with those of the wash-off test.[41]

Mechanical Properties

F_0 sensed by the load cell as the probe was compressing the formulations was lowest in G1, followed by G2 and G3, respectively [Figure 6(a)]. F_0 provided information about firmness of the formulations. F_r is the residual force obtained after the subsequent exponential decay of F_0 with respect to time. The results indicate that the firmness of the formulations was in the order G1 < G2 < G3. The higher firmnesses of G2 and G3 were attributed to the filler effect exerted by the presence of the internal phase. Similar effects were also observed by Firoozman and Rousseau.[42]

SR was calculated from the following equation:

$$\mathrm{SR}(\%) = \frac{F_0 - F_t}{F_0} \times 100 \tag{3}$$

The percentage SR was in the order G1 < G2 < G3. In general, a lower percentage SR corresponds to a higher elastic component in the formulations. Conversely, a lower percentage SR indicates a lower viscous component. The percentage SR results indicated that the incorporation of the internal phase resulted in a higher SR. G3 showed a higher SR compared to G2. This suggested that the viscous component was higher in G3 as compared to G2, even though G3 showed a higher firmness. This could be explained by the fact that the firmness was related to the instantaneous force exerted by the formulation when a load was applied, whereas SR was related to the rearrangement of the structure at the molecular level after a load was applied. The SR of the formulations was less than 10%; this indicated a predominant elastic behavior of the formulations. Similar observations were also observed by the calculation of the normalized residual force (F^*), which showed the occurrence of F^* in the order G1 > G2 > G3 [Figure 6(b)]. F^* provides information about the viscoelastic properties of formulations. F^* varies in the range 0–1, where an F^* value of 1

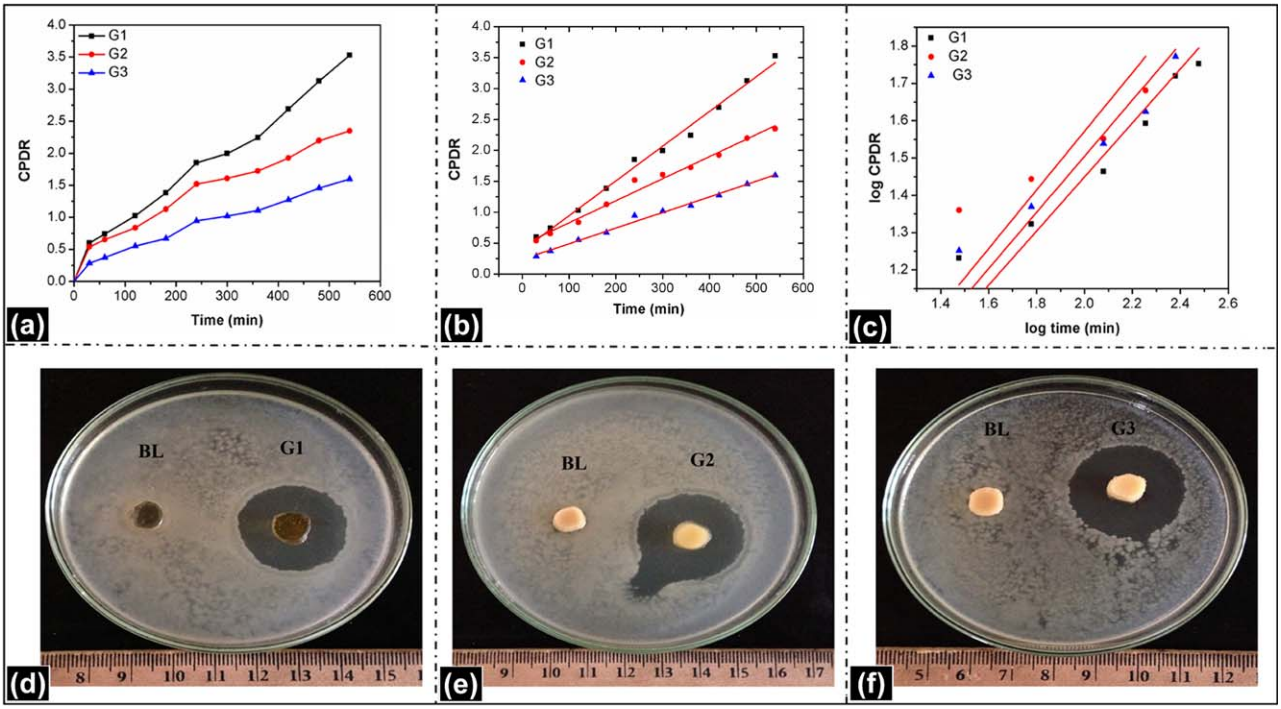

Figure 9. Drug-release studies: (a) drug-release profile, (b) zero-order release model, and (c) KP diffusion model. Antimicrobial efficiency of (d) G1, (e) G2, and (f) G3 (where BL represents the blank formulations without adding drug). [Color figure can be viewed in the online issue, which is available at wileyonlinelibrary.com.]

suggests a pure elastic formulation and an F^* value of 0 suggests a pure viscous formulation. The F^* values of the formulations was in the range $0.9 < F^* < 1.0$.

Creep and recovery studies were carried out for 10 cycles. After the completion of 10 cycles, all of the formulations were intact, and they were not completely deformed. The cyclic creep data was fitted with the four-element Burger's model:

$$J_c(t) = J_0 + J_1[1 - \exp(-t/t_1)] + t/\eta_0 \quad (4)$$

where $J_c(t)$ is the creep compliance at time t, J_0 is the instantaneous creep compliance, J_1 is the delayed or retarded compliance, t_1 is the retardation time, and η_0 is the pure viscosity of the material.

The creep compliance was calculated as the ratio of the strain to the applied stress [Figure 6(c)]. In general, J_0 and J_1 are proportional to the inverse of the storage modulus and the loss modulus of the materials. The changes in the viscosity and storage and loss moduli of the formulations at each cycle were calculated with Burger's model [Figure 6(d–f)]. A similar kind of trend was observed in all of the formulations. With the increase in the number of creep cycles, the viscosity and storage modulus of the formulations were reduced, whereas the loss modulus was increased. The curves of the storage and the loss moduli did not crossover. This suggested the absence of a gel-to-sol transition in the formulations during the study.

Thermal Properties

The thermal profile of the formulations was studied with a differential scanning calorimeter. The formulations showed a broad endothermic peak. The peaks were present at about 84, 86, and 129.7°C for G1, G2, and G3, respectively (Figure 7). The occurrence of the aforementioned peaks was due to the evaporation of water from the formulations.[43] No other peaks were visualized in G1 and G2 within the experimental scanning range. G3 showed an endothermic peak (shown by a circle) at about 52°C. The peak was due to the melting endotherm of the SO OG, which also showed an endothermic peak at about 52°C. This indicated that the physical properties of the OGs were not

Table III. Drug-Release Studies of the Formulations

Sample	CPDR	Zero order	KP model		Type of release
		R^2	R^2	n value	
G1C	3.52	0.991	0.999	0.503	Non-Fickian diffusion
G2C	2.34	0.983	0.957	0.396	Fickian diffusion
G3C	1.59	0.991	0.999	0.501	Non-Fickian diffusion

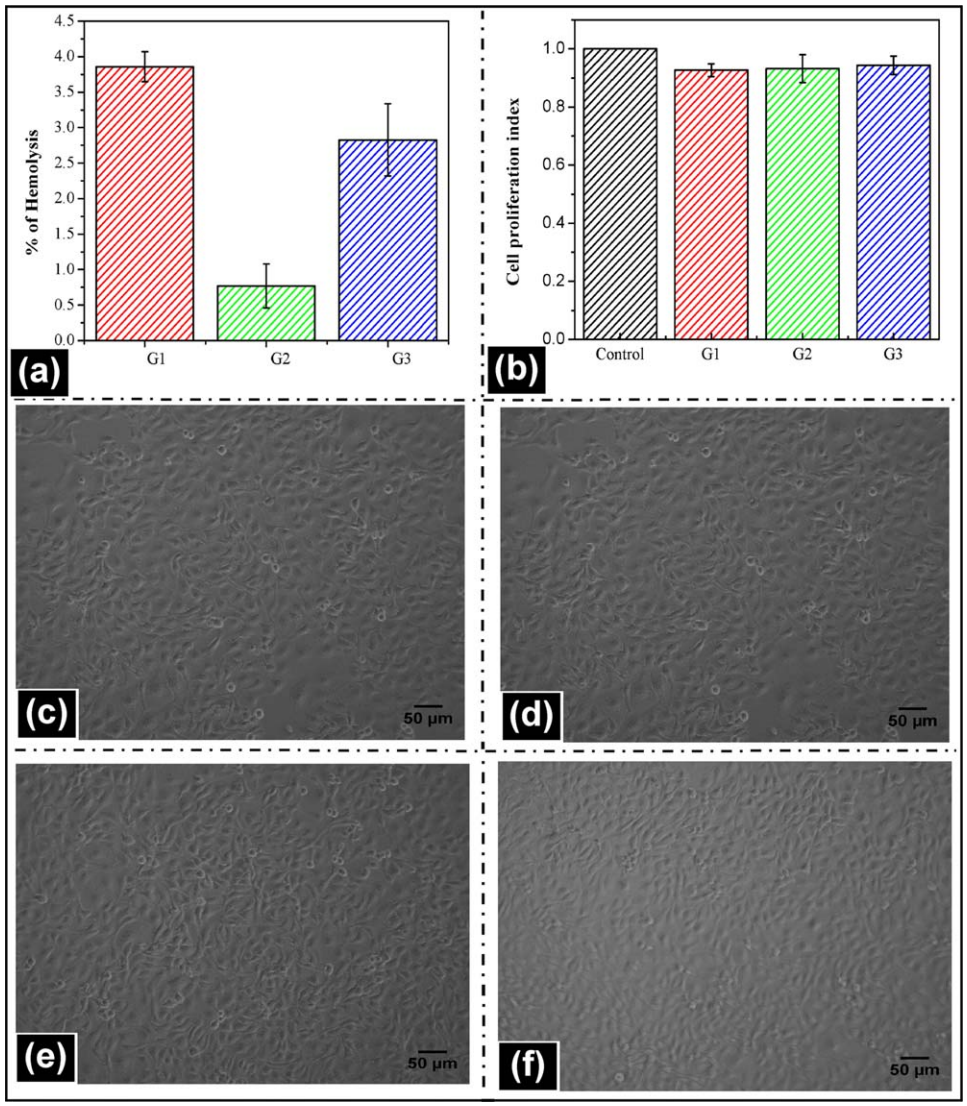

Figure 10. Biocompatibility studies: (a) hemocompatibility and (b) HaCaT cell viability index and cell morphology of the (c) control, (d) hydrogel, (e) emulgel, and (f) bigel. [Color figure can be viewed in the online issue, which is available at wileyonlinelibrary.com.]

changed after entrapment within the gelatin gel to form the bigel.[44]

Impedance Analysis

The Nyquist plot of the formulations did not show any formation of a semicircular region within the experimental conditions [Figure 8(a)]. This was attributed to the highly conductive nature of the formulations, which was due to presence of the external aqueous phase. The intersection of the Z'–Z'' plot (where Z' and Z'' are real and imaginary components of impedance, respectively) to the Z' axis was regarded as the bulk resistance. The bulk resistances of G1, G2, and G3 were found to be 58.4, 85.4, and 89.3 Ω, respectively. The increase in the bulk resistance was due to the incorporation of the SO and the SO OG within the gelatin matrix. The internal phase acted as the dielectric material. All of the formulations showed a relaxation peak at 100 kHz [Figure 8(b)]. In general, the tan δ profile was associated with the molecular relaxation of the polymer matrix. Because all of the formulations contained the gelatin matrix as the continuum phase, there was no significant change in the tan δ profile. The ac conductivity of the formulations showed an initial linear increase in the conductivity followed by a plateau phase [Figure 8(c)]. This kind of behavior is often associated with capacitive electrical components. The appearance of the capacitive behavior of G1 was explained by the electrode–sample interface polarization effect, which was negligible at higher frequencies. Although the profiles in G2 and G3 were due to the combined effects of the electrode–sample interface polarization effect and sample properties, the results suggest that the polarization effect was minimal at frequencies of 10 kHz or greater. Hence, the I–V characteristics of the formulations were determined at 10 kHz. The I–V plots were found to be linear [Figure 8(d)]. The slope of the I–V plots were found to be 0.181, 0.364, and 0.435 for G1, G2 and G3, respectively. The slopes gave an indication about the impedance of the formulations. The trend of the

results were in accordance with the results obtained from the Nyquist plot.[45]

Drug-Release Studies

The *in vitro* drug-release profiles of ciprofloxacin from the formulations are shown in Figure 9(a). The release study was carried out at pH 1.2 for 2 h and then at pH 7.2 for 7 h. At the end of the study, G1 showed the highest cumulative percentage drug release (CPDR), followed by G2 and G3, respectively (Table III). The trend of the release of the drugs was in direct relation to the electrical conductivity and swelling behavior of the formulations.[46] The release kinetics of the drugs were estimated by the fitting of various models, namely, the zero-order, first-order, and Higuchi models. The correlation coefficient values of the model fittings suggested that the best fit model was that of zero-order kinetics [Figure 9(b)]. The zero-order kinetics model is shown by a reservoir-type delivery vehicle. Hence, the developed formulations were regarded as reservoir-type delivery vehicles. The *n*-value (diffusion coefficient) was calculated from the Korsmeyer-Peppas (KP) model [Figure 9(c)]. The results suggest that G2C showed Fickian diffusion, whereas G1C and G3C showed non-Fickian diffusion-mediated drug release.[47]

The qualitative drug-release study from the formulations were studied by the determination of the antimicrobial efficiency of the formulations against *E. coli*. The zone of inhibition (an indicator of antimicrobial efficiency) was found to be similar in all of the formulations [Figure 9(d–f)].

Biocompatibility Studies

The preliminary biocompatibility of the formulations was tested by a hemocompatibility test. The test was used to measure the percentage of red blood cells damaged (percentage hemolysis) in the presence of the formulations. The damaged red blood cells released hemoglobin to the aqueous continuum phase, which in turn, resulted in a yellowish coloration. The falcon tubes were centrifuged, and the supernatant was collected.[48] The yellowish color was measured spectrophotometrically in the supernatant. The higher the optical density of the supernatant was, the greater the cell damage was. The percentage hemolysis in the presence of the developed formulations was found to be less than 5% [Figure 10(a)]. This suggested the probable biocompatible nature of the developed hydrogels.

The proliferation index of the HaCaT cells in the presence of the leachants is shown in Figure 10(b). The variations in the proliferation indices of the formulations were found to be statistically insignificant ($p > 0.05$) compared to those in the control. Also, there were no visual differences in the morphology of the cells in the presence of the leachants [Figure 10(c–f)]. This suggested that the leachants did not have any detrimental effects on the proliferation of the cells and, thereby, indicated the biocompatible nature of the prepared formulations.

CONCLUSIONS

In this article, we describethe comparison of the properties of a gelatin-based hydrogel, emulgel, and bigel. XRD and FTIR studies suggested that the incorporation of the SO and SO OGs within the gelatin matrix resulted in increases in the crystallinity. This resulted in increases in the mechanical properties of the emulgel and the bigel. The impedances of the emulgel and the bigel were higher. The swelling indices were lower in the emulgel and the bigel. The drug release from the formulations was found to be diffusion-mediated. The formulations showed sufficient antimicrobial properties for use in the delivery of antimicrobial drugs.

ACKNOWLEDGMENTS

The authors acknowledge financial support from the National Institute of Technology, Rourkela, and funds leveraged from a project sanctioned by the Department of Biotechnology, Government of India (BT/220/NE/TBP/2011), during the completion of the research.

REFERENCES

1. Singh, V. K.; Pal, K.; Pradhan, D. K.; Pramanik, K. *J. Appl. Polym. Sci.* **2013**, *130*, 1503.
2. Pal, K.; Singh, V. K.; Anis, A.; Thakur, G.; Bhattacharya, M. K. *Polym.–Plast. Technol. Eng.* **2013**, *52*, 1391.
3. Khade, S.; Behera, B.; Sagiri, S.; Singh, V.; Thirugnanam, A.; Pal, K.; Ray, S.; Pradhan, D.; Bhattacharya, M. *Iranian Polym. J.* **2014**, *23*, 171.
4. Gao, X.; He, C.; Xiao, C.; Zhuang, X.; Chen, X. *Polymer* **2013**, *54*, 1786.
5. Pal, K.; Banthia, A.; Majumdar, D. *African J. Biomed. Res.* **2006**, *9*, 23.
6. Adelmann, H.; Binks, B. P.; Mezzenga, R. *Langmuir* **2012**, *28*, 1694.
7. Dickinson, E. *Food Hydrocolloids* **2012**, *28*, 224.
8. Chen, H.; Chang, X.; Du, D.; Li, J.; Xu, H.; Yang, X. *Int. J. Pharm.* **2006**, *315*, 52.
9. Haigh, R. *Int. J. Food Sci. Technol.* **1978**, *13*, 491.
10. Baglio, V.; Girolamo, M.; Antonucci, V.; Aricò, A. *Int. J. Electrochem. Sci.* **2011**, *6*, 3375.
11. Mohamed, H.; Awatif, I. *Food Chem.* **1998**, *62*, 269.
12. Hoffman, A. S. *Adv. Drug Delivery Rev.* **2002**, *54*, 3.
13. Estroff, L. A.; Leiserowitz, L.; Addadi, L.; Weiner, S.; Hamilton, A. D. *Adv. Mater.* **2003**, *15*, 38.
14. Sagiri, S. S.; Pal, K.; Basak, P. *J. Appl. Polym. Sci.* **2014**, *131*, 40910.
15. Ricciardi, R.; Auriemma, F.; De Rosa, C.; Lauprêtre, F. *Macromolecules* **2004**, *37*, 1921.
16. Mansur, H. S.; Sadahira, C. M.; Souza, A. N.; Mansur, A. A. *Mater. Sci. Eng. C* **2008**, *28*, 539.
17. Gupta, P.; Vermani, K.; Garg, S. *Drug Discovery Today* **2002**, *7*, 569.
18. Ludwig, A. *Adv. Drug Delivery Rev.* **2005**, *57*, 1595.
19. Jones, D. S.; Woolfson, A. D.; Brown, A. F. *Int. J. Pharm.* **1997**, *151*, 223.
20. Hurler, J.; Engesland, A.; Poorahmary Kermany, B.; Škalko-Basnet, N. *J. Appl. Polym. Sci.* **2012**, *125*, 180.

21. Anseth, K. S.; Bowman, C. N.; Brannon-Peppas, L. *Biomaterials* **1996**, *17*, 1647.
22. Otake, K.; Inomata, H.; Konno, M.; Saito, S. *Macromolecules* **1990**, *23*, 283.
23. Singh, V. K.; Sagiri, S. S.; Pal, K.; Khade, S. M.; Pradhan, D. K.; Bhattacharya, M. K. *J. Appl. Polym. Sci.* **2014**, *131*, DOI: 10.1002/app.40445.
24. Jalani, N. H.; Ramani, M.; Ohlsson, K.; Buelte, S.; Pacifico, G.; Pollard, R.; Staudt, R.; Datta, R. *J. Power Sources* **2006**, *160*, 1096.
25. Singh, V. K.; Ramesh, S.; Pal, K.; Anis, A.; Pradhan, D. K.; Pramanik, K. *J. Mater. Sci. Mater. Med.* **2014**, *25*, 703.
26. Paulsson, M.; Edsman, K. *Pharm. Res.* **2001**, *18*, 1586.
27. Mallick, S.; Sagiri, S.; Singh, V.; Pal, K.; Pradhan, D.; Bhattacharya, M. *Polym.–Plast. Technol. Eng.* **2014**, *53*, 700.
28. Amarnath, L. P.; Srinivas, A.; Ramamurthi, A. *Biomaterials* **2006**, *27*, 1416.
29. Pal, K.; Banthia, A. K.; Majumdar, D. K. *AAPS PharmSciTech.* **2007**, *8*, 142.
30. Nakao, A.; Nagaoka, S.; Mori, Y. *J. Biomater. Appl.* **1987**, *2*, 219.
31. Lee, S. J.; Yhee, J. Y.; Kim, S. H.; Kwon, I. C.; Kim, K. *J. Controlled Release* **2013**, *172*, 358.
32. Lee, K. Y.; Mooney, D. *J. Chem. Rev.* **2001**, *101*, 1869.
33. Peppas, N. A.; Mikos, A. G. *Hydrogels Med. Pharm.* **1986**, *1*, 1.
34. Ohya, S.; Kidoaki, S.; Matsuda, T. *Biomaterials* **2005**, *26*, 3105.
35. Reichelt, R.; Schmidt, T.; Kuckling, D.; Arndt, K. F. *Macromol. Symp.* **2011**, *36*, 1184.
36. Lee, W. F.; Fu, Y. T. *J. Appl. Polym. Sci.* **2003**, *89*, 3652.
37. Shapiro, Y. E. *Prog. Polym. Sci.* **2011**, *36*, 1184.
38. Shu, C.; Xianzhu, Y.; Zhangyin, X.; Guohua, X.; Hong, L.; Kangde, Y. *Ceram. Int.* **2007**, *33*, 193.
39. Kou, J. H.; Amidon, G. L.; Lee, P. I. *Pharm. Res.* **1988**, *5*, 592.
40. Sagiri, S. S.; Sethy, J.; Pal, K.; Banerjee, I.; Pramanik, K.; Maiti, T. K. *Des. Monomers Polym.* **2013**, *16*, 366.
41. Thirawong, N.; Nunthanid, J.; Puttipipatkhachorn, S.; Sriamornsak, P. *Eur. J. Pharm. Biopharm.* **2007**, *67*, 132.
42. Firoozmand, H.; Rousseau, D. *Food Hydrocolloids* **2013**, *30*, 333.
43. Toro-Vazquez, J.; Morales-Rueda, J.; Dibildox-Alvarado, E.; Charo-Alonso, M.; Alonzo-Macias, M.; González-Chávez, M. *J. Am. Oil Chem. Soc.* **2007**, *84*, 989.
44. Kulmyrzaev, A.; Bryant, C.; McClements, D. J. *J. Agric. Food Chem.* **2000**, *48*, 1593.
45. Walter, G. *Corros. Sci.* **1986**, *26*, 681.
46. Sagiri, S. S.; Behera, B.; Sudheep, T.; Pal, K. *Des. Monomers Polym.* **2012**, *15*, 253.
47. Cassidy, C. M.; Tunney, M. M.; McCarron, P. A.; Donnelly, R. F. *J. Photochem. Photobiol. B: Biol.* **2009**, *95*, 71.
48. Říhová, B. *Adv. Drug Delivery Rev.* **1996**, *21*, 157.